Terahertz Band Demands Ultra-Broadband Waveform: An Analysis of Phase Noise Estimation and Compensation

Michael Wilder[1], Ryan Primus[1], Hisham Kholidy[2], Arjun Singh[1], and Priyangshu Sen[1]
[1] Electrical and Computer Engineering, [2]Network and Computer Security, SUNY Polytechnic Institute
Utica, NY, 13502,USA
{wilderm,primusr,kholidh,singha8,senp}@sunypoly.edu

Abstract

One of the challenges in the development of effective next-generation, 6G and beyond, wireless systems in the terahertz (0.1-10 THz) band is the high phase noise (PN) that arises from non-linear distortions in the local oscillator (LO). This is further magnified due to the use of a high number of frequency multipliers to reach the THz carrier frequency. This paper explores the performance of novel PN estimation and compensation techniques in aggravated PN scenarios, which are possible in the THz band. Exhaustive numerical simulations utilizing an in-house developed PN generator are utilized to analyze the effect of several frame parameters, including symbol rate, pilot separation, and pilot length, on PN tracking and compensation techniques. It is shown that large pilot length and low bandwidth utilization can impede PN estimation, laying the foundation for addressing the challenges associated with PN in THz-band communication and providing insights into the effective strategies for PN estimation and compensation.

CCS Concepts

• **Networks → Link-layer protocols**.

Keywords

THz-communication, ultra-broadband, phase noise modeling, compensation, link reliability

1 Introduction

The escalating need for high data rates in next-generation wireless communication systems, including 6G and beyond, has necessitated the development of a network that can handle data rates ranging from hundreds of gigabits to terabits per second links [2]. Besides communication, there is also an increasing demand for high-resolution sensing in the sub-millimeter to micro-meter range for precise vital tracking, automotive, and aviation sensing and imaging applications. These needs demand the exploration of new spectrum technology for ultra-broadband bandwidth ranging from tens to hundreds of gigahertz. The availability of such massive chunks of bandwidth in the terahertz (0.1-10 THz) band, has led to THz-band technology being considered a critical technology for next-generation wireless systems [1].

Currently, significant strides have been made in research and development efforts aimed towards technological advancements in the successful utilization of the THz band. However, high spreading/path loss limits communication range and reduces SNR. Further, the varying channel multipath characteristics with slight environmental changes and device impairments also affect link reliability. All these, eventually, adversely impact the performance [5, 8, 12].

Path losses can be countered through commercially available high-gain antennas, and channel state estimation techniques are evolving for the dynamic channel [12]. Nonetheless, several issues remain in the case of device impairments. One such crucial phenomenon is Phase noise (PN), which affects the phase component of the information-bearing modulated signal, resulting in a degradation of the information's integrity and limiting the achievable data rates [6]. Specifically, PN is a pink noise that arises due to time-domain instability, known as jitter, of the local oscillator (LO). This issue is particularly exacerbated when the LO signal is converted to sub-THz (0.1-0.3 THz) and THz (0.3-10 THz) carrier frequency ranges through a high number of multiplier chains, as are commonly utilized. Thus, careful consideration and mitigation of PN is essential for optimal performance. In the frequency domain, PN is expressed by comparing it with the carrier power at various offset frequencies from the carrier frequency. It is more concentrated in the frequency components closer to the carrier frequency (lower offset), and thus fluctuates slower than regular additive white Gaussian noise (AWGN), showing a strong correlation with the neighboring values. This makes it possible to track PN through pilot symbols [3].

The estimation and compensation of PN in both single and multi-carrier systems have been the subject of several studies. For multicarrier systems, in the case of 5G-NR, phase tracking reference signals (PTRS) are used to estimate and compensate for PN in orthogonal frequency division multiplexing (OFDM) systems [10]. The work in [15] suggests increasing the bandwidth as a possible way to mitigate the additional inter-carrier interference for OFDM systems caused by PN. Moreover, the Orthogonal Time Frequency Space (OTFS) framework employs the delay-doppler coordinate system to effectively mitigate the adverse impact of PN [4]. However, multicarrier schemes have a high PAPR, limiting their use at THz frequencies [11], as it may cause THz-frequency power amplifiers to operate in a state of saturation, severely limiting the power output. In single-carrier communication systems, it is customary to deploy pilots to aid in the tracking and compensation of PN [17]. However, the effectiveness of this particular approach in the context of THz-band systems remains an area of limited exploration. It is important to note that PN does not exert as significant an impact on millimeter wave (24-60 GHz) and sub-6 GHz systems as it does on THz-band systems. Our prior work in [16] proposed a THz spread spectrum technique that balanced data rate and PN by sacrificing possible throughput.

The present article presents a numerical study that examines critical novel aspects for efficiently dealing with PN at THz frequencies. These include i) high-phase noise scenarios that may arise in Thz band systems [13, 14]; ii) the effect of symbol rate on PN tracking and compensation; iii) the effect of pilot separation on PN tracking and compensation; and iv) the effect of the length of the pilot symbols on PN tracking and compensation. The findings reveal significant

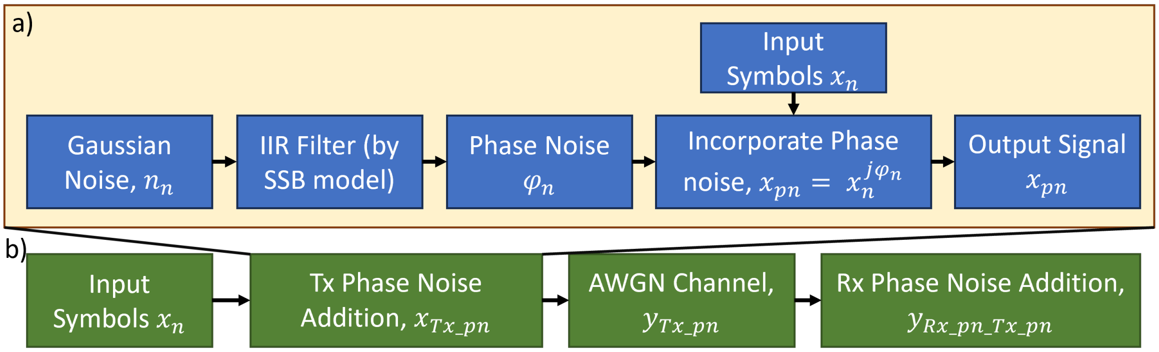

Figure 1: System model: a) Phase noise simulation model to incorporate PN with the input signal, and b) End-to-end system model that encompasses both transceiver PN and AWGN.

observations that highlight the relevance of addressing PN related issues in the design of a THz system. One interesting observation is that the PN of a low baseband bandwidth system operating at these high carrier frequencies cannot be reduced efficiently.

The rest of the paper is organized as follows. First, in Section 2, we provide our system model and provide a detailed explanation of the properties of PN. In Section 3, we introduce and explain the proposed PN estimation and compensation technique. We thoroughly evaluate the performance of the proposed scheme via numerical analyses in Section 4. Finally, we conclude our paper in Section 5, and outline a roadmap for future work.

2 System Model

This section presents an overview of PN and its effect on the THz-band communication system. Further, we provide details of our end-to-end system model in examining the performance of the link when subjected to PN. We utilize a baseband equivalent setup to emulate the PN through an in-house developed model.

2.1 Phase Noise

PN is a transient, stochastic fluctuation in the phase of an oscillator caused by instability in the time domain known as jitter [7]. In the frequency domain, it is common to express this effect as single-sideband (SSB) PN. Specifically, the PN, which is power leakage in frequency per hertz bandwidth at different frequency offsets from the carrier component, is compared with carrier power and represented in dBc/Hz.

Moreover, It is possible to obtain the approximated equivalent PN at the carrier, f_c, by shifting the PN at the local oscillator (LO), f_{LO}, frequency by $SSB_{\text{shift}} = 20\log_{10}(f_c/f_{LO})$, which is similar to shifting by $SSB_{\text{shift}} = 20\log_{10}(Mul)$. Mul is number of multipliers used to up-convert LO signal to carrier signal. A significant number of multiplier chains need to be employed to acquire the carrier frequency at the THz band. As is evident, this exacerbates the PN statistics and necessitates the implementation of an appropriate estimation and compensation methodology.

2.2 End-to-end System Model

The simulation setup is divided into two parts – i) phase noise generation and ii) communication model, as summarized in Figure 1. For PN generation, as shown in Figure 1(a), we employ a Gaussian noise subject to an infinite impulse response (IIR) filter derived from a single-sideband (SSB) PN measurement conducted at a 120 GHz carrier frequency [9]. We compare the simulated PN with the actual experimental PN obtained from experimentation in [9]. As depicted in Figure 2, the simulated values exhibit a close match with the experimental values, thereby serving to validate the accuracy of our in-house model for PN generation. The PN distorted symbols, x_{pn}, are attained through the integration of the input signal samples, x_n, with the PN, ϕ_n, and given by

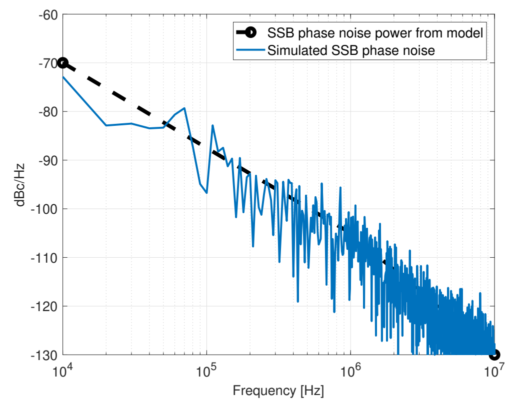

Figure 2: SSB Phase noise for 120 GHz system obtained from [9] and simulated SSB PN.

$$x_{pn} = x_n^{j\phi_n}. \tag{1}$$

In the communication model, as shown in Figure 1(b), we consider an additive AWGN channel with 30 dB signal-to-noise ratio (SNR) featuring a line of sight (LOS) link and a single-input, single-output (SISO) antenna system. This allows us to focus solely on the PN performance. Further, to mimic the transmitter and receiver multiplier chain PN impairment, we incorporate PN twice into the system following the PN generation model. The end output of the simulation system is represented by $y_{Rx\_pn\_Tx\_pn}$.

3 Phase Noise Estimation and Compensation

The phenomenon of PN is characterized by its slow-changing nature over time. This is because the strongest PN powers are concentrated in the vicinity of the carrier (low off-set frequency), as indicated

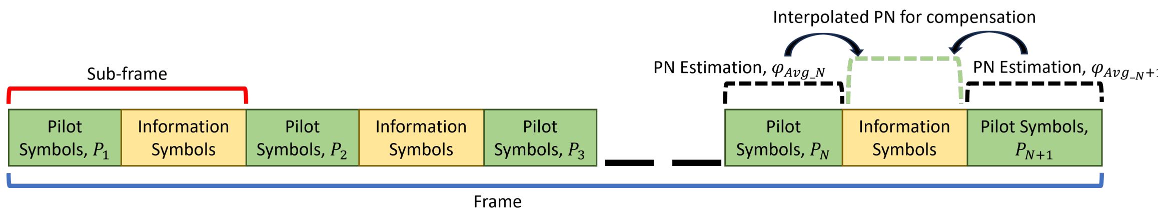

Figure 3: Proposed frame and sub-frame structure for estimation and compensation of the PN.

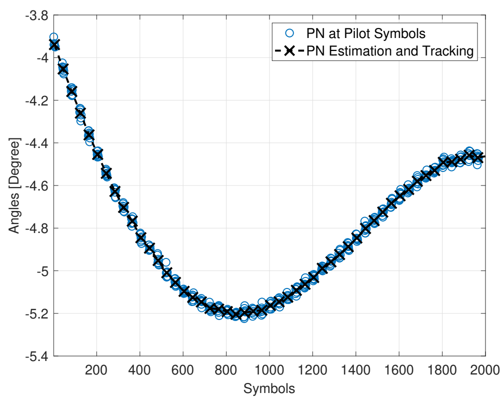

Figure 4: PN Estimation and tracking through the known pilot symbols with 30 GHz symbol-rate signal, sub-frame consisting 8 pilot and 32 information symbols, and starting PN of -55 dBc/Hz at 10KHz.

in Figure 2. Therefore, the noise is trackable through pilot symbols known to the receiver, which can be observed in Figure 4. In this specific scenario, we have employed 8 pilot symbols, interspersed with 32 information symbols. The known pilot symbols are utilized to determine the average estimated PN, while linear interpolation is employed to track the PN for compensation purposes for information symbols. To incorporate this scheme into the communication system, we propose to divide the frame into sub-frames, with each sub-frame containing pilot symbols for PN estimation. This approach ensures that pilot symbols are present on both ends of the sub-frame, as illustrated in Figure 3. The pilots are utilized to determine the estimated phase distortion resulting from PN at the start, ϕ_{Avg_N}, and end, ϕ_{Avg_N+1}, of the Nth sub-frame and is given by

$$\phi_{Avg\_N} = angle(\frac{1}{n}\hat{P_N}.\hat{P_{Nr}}^H), \text{and} \quad (2)$$

$$\phi_{Avg\_N+1} = angle(\frac{1}{n}\hat{P_{N+1}}.\hat{P_{(N+1)r}}^H). \quad (3)$$

Here, $\hat{P_N} = [P_N(1)P_N(2)...P_N(n)]$ is a column vector made with transmitted pilot symbols at the beginning of the Nth sub-frame and $\hat{P_{N+1}}$ is the similar column vector at the end of the sub-frame. $\hat{P_{Nr}}$ and $\hat{P_{(N+1)r}}$ represent the received column vector correspond to $\hat{P_N}$ and $\hat{P_{N+1}}$, respectively. Here, n is the number of pilot symbols utilized to estimate the average PN. The process of estimating phase distortions within information symbols involves utilizing the calculated average phase distortions at both ends and performing linear interpolation

Metrics	Value
PN level (10 KHz offset)	-70 to -35 dBc/Hz
Symbol rates	1MHz to 30 GHz
Length of sub-frames	256 to 8192
length of pilot symbols	16 to 64

Table 1: Values of different metrics for simulation.

for values in between, and is given by

$$\phi_X(x') = \frac{x' - x_{PN}}{x_{P(N+1)} - x_{PN}}(\phi_{Avg\_N+1} - \phi_{Avg\_N}) + \phi_{Avg\_N}. \quad (4)$$

Here $\hat{\phi_X} = [\phi_X(1)\phi_X(2)...\phi_X(x)]$ is the interpolated PN that is being utilized for compensation of the phase distortion in information symbols. Here, x represents the number of information symbols in the sub-frame. x' represents the position of the information symbol with respect to x_{PN}, which is the end position of the pilot at the front, and $x_{P(N+1)}$ indicates the start position of the pilot at the end of Nth sub-frame. The process of PN estimation and tracking mechanism is depicted in Figure 3, following which, the phase compensated information symbols, y_c, are obtained as

$$y_c(x') = y_{Rx\_pn\_Tx\_pn}(x')^{-j\phi_X(x')}. \quad (5)$$

4 Results

In this section, we compare the performance of estimation and compensation schemes in terms of bit error rate (BER) considering PN, taking into account various PN levels, different symbol rates of the waveform, sub-frame lengths by increasing the number of information symbols, and pilot symbols lengths as shown in Table 1. In fact, we increase the PN power level equally on all the relevant offset frequencies, while the noise floor is kept constant at -180 dBc/Hz (at an offset of 20 MHz from the carrier). Binary phase shift keying (BPSK) modulation is used for both information and pilot bits to enable clearer observation and express the severity of the PN. The pilot bits are selected from a pseudo-random code. The simulation results are shown in Figure 5 and illustrate the variations' impact on BER.

4.1 Effect of Symbol Rate on Phase Compensation

Upon comparison of Figure 5(a) and (b), it is evident that the estimation and compensation technique for PN is both effective and essential for maintaining link reliability. Added, it is noteworthy that higher symbol rate waveforms exhibit significantly better responses to the estimation, tracking, and compensation techniques. As an example, the BER is three orders lower at 30 GHz compared to the 1 MHz symbol rate signals (Figure 5(a)). This is due to the fact that

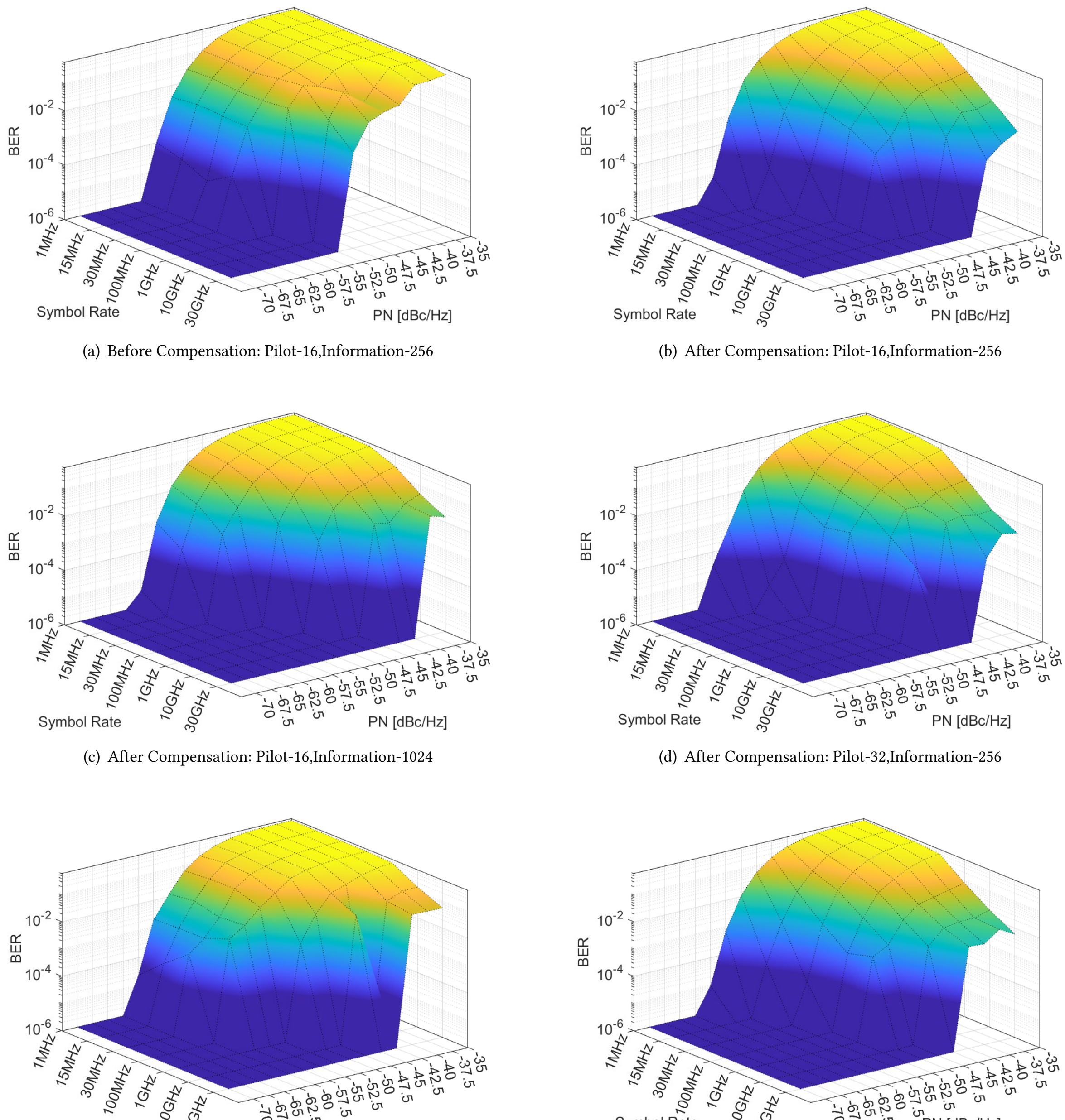

(a) Before Compensation: Pilot-16,Information-256

(b) After Compensation: Pilot-16,Information-256

(c) After Compensation: Pilot-16,Information-1024

(d) After Compensation: Pilot-32,Information-256

(e) After Compensation: Pilot-16,Information-8192

(f) After Compensation: Pilot-64,Information-256

Figure 5: Comparison of the performance of PN estimation and compensation scheme is tested under different metrics.

higher symbol rate waveforms possess a lower wavelength in time, resulting in a lower sub-frame duration in comparison to lower symbol rate counterparts. Consequently, tracking and compensating the PN becomes easier, given that the PN changes slowly and exhibits a high correlation to neighboring values.

4.2 Effect of Increasing Sub-Frame Length

The scheme's effectiveness is reduced with an increase in the length of sub-frames through the addition of more information symbols between the pilots. As the separation between the pilots increases, the system loses its ability to track the PN effectively, and the BER increases. Through simulations, we observed that a slight change in sub-frame length and time duration does not have a significant effect. However, beyond a certain point, the BER increases significantly, as evidenced in Figure 5(b), (c), and (e). A slight change in BER was observed from a sub-frame length of 256 to 1024 symbols, whereas a significant change was noted for a sub-frame length of 8192.

4.3 Effect of Increasing Pilot Length

Increasing the length of the pilot symbol has a lower significance in tracking the PN. In Figure 5(b), (d), and (f), the length of pilot symbols are 16, 32, and 64, respectively, and as we increase the pilot bits, the BER increases slightly. If we only consider the PN scenario, increasing the length of pilot symbols has a negative impact. This is because longer pilot symbols shift the average point, leading to an increase in tracking error, i.e., error in between actual PN within information bits and tracked PN by the estimation algorithm. We estimate a high SNR (30 dB), resulting in low AWGN. Therefore, the length of pilot bits may have more significance in low SNR scenarios where smoothing of AWGN is also important.

4.4 Discussion

As the modulation order increases, there arises a pressing need for precise estimation and compensation techniques for PN. The BER increases with higher-order modulation due to the diminishing phase separation between constellation points, even with the same level of PN. Consequently, it becomes crucial to utilize waveforms with wide bandwidth, ranging from a few GHz to tens of GHz, and high-symbol rates. Additionally, a sub-frame structure with a small size can be a useful tool in tracking PN effectively. A judicious selection of pilot length may serve to ameliorate the effects of PN fluctuations, as well as AWGN. It is, however, important to note that the selection process requires a trade-off between the system's reliability and throughput. In order to attain optimal performance, careful consideration should be given to the pilot length, as this selection may have a significant impact on the overall performance of the system. In all cases, a high symbol rate in the range of tens of GHz is an indispensable requirement for better system performance. It is safe to assert that single carrier THz band signals necessitate an ultra-broadband waveform design that supports high data rates.

5 Conclusion

The present paper aims to underscore the significance of employing the PN estimation and compensation technique for single-carrier THz-band communication systems. It is demonstrated that higher symbol rate and the use of ultra-broadband waveform are instrumental in mitigating the PN and maintaining link reliability. Further, the paper emphasizes the critical role of selecting appropriate pilot symbols' separation and length in mitigating the PN while maintaining throughput. These findings have practical implications that can considerably enhance the performance of THz wireless systems.

In light of this, we plan to test the scheme in practical scenarios in real testbed. Further, we would like to evaluate the performance of higher-order modulation with multicarrier schemes in the presence of high AWGN and multipath THz channels. We plan to use AI/ML algorithms to track PN and optimize frame structure for maximum throughput while ensuring link reliability. Further, we intend to enhance security using artificially generated PN from our in-house model.

Acknowledgments

The authors acknowledge the funds from the SUNY Poly state seed grants and WINGS center support at SUNY Poly.

References

[1] I. F. Akyildiz, J. M. Jornet, and Chong Han. 2014. Terahertz band: Next frontier for wireless communications. *Physical Communication (Elsevier) Journal* 12 (Sept. 2014), 16–32.

[2] Ian F Akyildiz, Ahan Kak, and Shuai Nie. 2020. 6G and beyond: The future of wireless communications systems. *IEEE access* 8 (2020), 133995–134030.

[3] Shaohua Chen, Yang Gao, and Tao Lin. 2017. Effect and mitigation of oscillator vibration-induced phase noise on carrier phase tracking. *GPS Solutions* 21 (2017), 1515–1524.

[4] Ronny Hadani and Anton Monk. 2018. OTFS: A new generation of modulation addressing the challenges of 5G. *arXiv preprint arXiv:1802.02623* (2018).

[5] Josep Miquel Jornet and Ian F Akyildiz. 2011. Channel modeling and capacity analysis for electromagnetic wireless nanonetworks in the terahertz band. *IEEE Transactions on Wireless Communications* 10, 10 (2011), 3211–3221.

[6] Mohammad Reza Khanzadi. 2015. *Phase Noise in Communication Systems–Modeling, Compensation, and Performance Analysis.* Chalmers University of Technology.

[7] Thomas H Lee and Ali Hajimiri. 2000. Oscillator phase noise: A tutorial. *IEEE journal of solid-state circuits* 35, 3 (2000), 326–336.

[8] Claire T Parisi, Sherif Badran, Priyangshu Sen, Vitaly Petrov, and Josep M Jornet. 2023. Modulations for Terahertz Band Communications: Joint Analysis of Phase Noise Impact and PAPR Effects. *IEEE Open Journal of the Communications Society* (2023).

[9] Michele Polese, Viduneth Ariyarathna, Priyangshu Sen, Jose V Siles, Francesco Restuccia, Tommaso Melodia, and Josep M Jornet. 2022. Dynamic spectrum sharing between active and passive users above 100 GHz. *Communications Engineering* 1, 1 (2022), 6.

[10] Yinan Qi, Mythri Hunukumbure, Hyungju Nam, Hyunil Yoo, and Saidhiraj Amuru. 2018. On the phase tracking reference signal (PT-RS) design for 5G new radio (NR). In *2018 IEEE 88th Vehicular Technology Conference (VTC-Fall)*. IEEE, 1–5.

[11] Priyangshu Sen, Viduneth Ariyarathna, and Josep M Jornet. 2022. An optimized M-ary amplitude phase shift keying scheme for ultrabroadband terahertz communication. In *2022 IEEE 19th Annual Consumer Communications & Networking Conference (CCNC)*. IEEE, 661–666.

[12] Priyangshu Sen, Sherif Badran, Vitaly Petrov, Arjun Singh, and Josep M Jornet. 2024. Impact of the Antenna on the Sub-Terahertz Indoor Channel Characteristics: An Experimental Approach. *arXiv preprint arXiv:2403.04168* (2024).

[13] Priyangshu Sen, Dimitris A Pados, Stella N Batalama, Erik Einarsson, Jonathan P Bird, and Josep M Jornet. 2020. The TeraNova platform: An integrated testbed for ultra-broadband wireless communications at true Terahertz frequencies. *Computer Networks* 179 (2020), 107370.

[14] Priyangshu Sen, Jose V Siles, Ngwe Thawdar, and Josep M Jornet. 2023. Multi-kilometre and multi-gigabit-per-second sub-terahertz communications for wireless backhaul applications. *Nature Electronics* 6, 2 (2023), 164–175.

[15] Jinwen Shentu, Kusha Panta, and Jean Armstrong. 2003. Effects of phase noise on performance of OFDM systems using an ICI cancellation scheme. *IEEE Transactions on Broadcasting* 49, 2 (2003), 221–224.

[16] Michael Wilder, Priyangshu Sen, and Arjun Singh. 2023. A Spread Spectrum Modulation Technique for THz Communications in the Presence of Phase Noise. In *IEEE Future Networks World Forum*. IEEE.

[17] Zhilin Zhang, Steven Loh, Shadi Abu-Surra, and Rakesh Taori. 2015. Mitigation of Phase Noise and Phase Rotation in Single-Carrier Communication Systems Using Pilots and Smoothing Technique. In *2015 IEEE International Conference on Ubiquitous Wireless Broadband (ICUWB)*. IEEE, 1–5.